AIAA JOURNAL
Vol. 32, No. 5, May 1994

Sensitivity Analysis and Optimal Design of Thin Shells of Revolution

C. M. Mota Soares* and C. A. Mota Soares†
CEMUL/IST—Centro de Mecânica e Materiais da Universidade Técnica de Lisboa, Lisboa 1096, Portugal
and
J. Infante Barbosa‡
Escola Náutica Infante D. Henrique, Oeiras 2780, Portugal

This paper presents the sensitivity analysis for the optimization of axisymmetric shells subjected to arbitrary loading. Thickness and shape design variables are considered. The model is based on a two-node frustum-cone finite element with 8 degrees of freedom based on Love-Kirchhoff assumptions. The objective of the design is the minimization of the volume of the shell material, the maximization of the fundamental natural frequency, the minimization of the maximum stresses, or the minimization of the maximum displacement. The constraint functions are the displacements, stresses, enclosed volume of the structure, volume of shell material or the natural frequency of a specified mode shape. The design sensitivities are calculated analytically, using a symbolic manipulator, semianalytically, and by global finite difference. The efficiency and accuracy of the models developed are discussed with reference to the applications.

Introduction

STRUCTURAL optimization of complex structures using finite element techniques requires the sequential use of structural and sensitivity analyses combined with a numerical optimizer. For a successful optimization the requirements are a good finite element model, adequate sensitivities, proper choice of objective function, design variables, constraints, and a suitable method of solution of the nonlinear mathematical problem.

This work presents a frustum-cone finite element model with 8 degrees of freedom, based on Love-Kirchhoff assumptions, for thin axisymmetric shell-type structures.[1] The sensitivities with respect to the design variables, namely, the thicknesses and/or radial nodal coordinates, are evaluated analytically, semianalytically, or by global finite difference.

The evaluation of sensitivities of structural response to changes in design variables is a crucial stage in the optimal design of complex structures, representing a major factor with regard to the computer time required for the optimization process. Hence it is important to have efficient techniques to calculate these derivatives. The simplest technique of evaluating sensitivities of response with respect to changes in design variables is through the finite difference approximation, called global finite difference, which is computationally expensive, or through the use of the semianalytical method[2–4] or the analytical method as described in the next section. These later methods can both be applied with the direct or adjoint structure technique for static-type situations.[5]

In this paper the formulation for the sensitivities of axisymmetric shells is presented for the general case of arbitrary loading. Other numerically based solutions are reported by Marcelin and Trompette[6] using a finite element with a two-node straight element and/or a three-node parabolic element based in Love-Kirchhoff shell theory associated with the semianalytical method to evaluate the sensitivities. Other authors, such as Plaut et al.[7] and Chenais,[8] present alternative theories and models for optimization of shell structures. Mehrez and Rousselet[9] presented the analysis and optimization of shells of revolution using Koiter's model with the implementation of B-splines for the middle surface and finite element for displacements. More recently, Bernardou et al.,[10] using only the general continuous formulation of the problems, presented a methodology for optimizing the shape (middle surface and thickness) of an elastic general thin shell under different criteria.

Since the strain field based on shell theory is usually more complex than alternative ones for planar and solid continuum elements, in the development of analytical sensitivities for shape design variables of shell structures, it is convenient in the majority of cases to use symbolic manipulators,[11] to overcome the complexity of the formulas involved. This approach is followed in the present work.

The formulation presented in this paper is applied to the minimum weight design of thin axisymmetric shell structures subjected to constraints on displacements, stresses, natural frequencies, volume of the shell material, and enclosed volume of the structure. A maximization of the natural frequency of a chosen vibration mode, the minimization of maximum displacement, or alternatively the minimization of maximum stresses using a bound formulation is carried out.

A comparative study of analytical vs semianalytical and global finite difference shows the advantage of analytical sensitivities with regard to the accuracy and the advantage of semianalytical sensitivities with regard to CPU time.

The automated design synthesis (ADS) program of Vanderplaats[12] is used to solve the nonlinear mathematical programming problem.

Sensitivity Analysis of Axisymmetric Shells

Analytical Method

For the present frustum-conical element (Fig. 1) the strain components for membrane and bending effects are given, as in Zienkiewicz[1] and Kraus,[13] by

$$\varepsilon^0 = \Delta_m U \tag{1}$$

$$\chi = \Delta_f U \tag{2}$$

Received Dec. 17, 1992; revision received Oct. 17, 1993; accepted for publication Oct. 18, 1993. Copyright © 1993 by the American Institute of Aeronautics and Astronautics, Inc. All rights reserved.

*Associate Professor, Departamento de Engenharia Mecânica, Av. Rovisco Pais. Member AIAA.

†Professor, Departamento de Engenharia Mecânica, Av. Rovisco Pais.

‡Assistant Professor, Departamento de Máquinas Marítimas, Paço de Arcos.

where the operators Δ_m and Δ_f are

$$\Delta_m = \begin{bmatrix} \frac{\partial}{\partial S} & 0 & 0 \\ \frac{\cos\phi}{r} & \frac{\sin\phi}{r} & \frac{1}{r}\frac{\partial}{\partial\theta} \\ \frac{1}{r}\frac{\partial}{\partial\theta} & 0 & \left(\frac{\partial}{\partial S} - \frac{\cos\phi}{r}\right) \end{bmatrix} \tag{3}$$

$$\Delta_f = \begin{bmatrix} 0 & -\frac{\partial^2}{\partial S^2} & 0 \\ 0 & -\frac{1}{r^2}\left(\frac{\partial^2}{\partial\theta^2} + r\cos\phi\frac{\partial}{\partial S}\right) & \frac{\sin\phi}{r^2}\frac{\partial}{\partial\theta} \\ 0 & \frac{2}{r^2}\left(\cos\phi\frac{\partial}{\partial\theta} - r\frac{\partial^2}{\partial S\partial\theta}\right) & \frac{2\sin\phi}{r^2}\left(r\frac{\partial}{\partial S} - \cos\phi\right) \end{bmatrix} \tag{4}$$

The displacement components u, w, and v, in the tangential, normal, and circumferential directions, respectively, are expanded in Fourier series of the type

$$U = \sum_{n=0}^{N} (C_n U_n + \hat{C}_n \hat{U}_n) \tag{5}$$

where

$$C_n = \begin{bmatrix} \cos n\theta & 0 & 0 \\ 0 & \cos n\theta & 0 \\ 0 & 0 & \sin n\theta \end{bmatrix}; \quad \hat{C}_n = \begin{bmatrix} \sin n\theta & 0 & 0 \\ 0 & \sin n\theta & 0 \\ 0 & 0 & -\cos n\theta \end{bmatrix} \tag{6}$$

$$U_n = \begin{bmatrix} u_n & w_n & v_n \end{bmatrix}^T; \quad \hat{U}_n = \begin{bmatrix} \hat{u}_n & \hat{w}_n & \hat{v}_n \end{bmatrix}^T \tag{7}$$

The first and second terms of Eq. (5) represent the components of displacements that are, respectively, symmetric and antisymmetric about $\theta = 0$ plane, where u_n, w_n, and v_n are the amplitudes of the symmetric part, $\hat{u}_n$, $\hat{w}_n$, and $\hat{v}_n$ are the amplitudes of the antisymmetric part for the harmonic n, and N is the total number of Fourier terms.

Considering for the sake of simplicity only the symmetric terms and assuming that the shape functions define the variation of displacements, the components of displacements can be written in a product form as

$$U_n = NLq_n^e \tag{8}$$

where q_n^e is the vector of the element nodal displacement amplitudes in the system referential, L is the transformation matrix that relates shell displacements with degrees of freedom of the element and system, and N is the matrix of shape functions.

Substituting Eq. (3–8) into Eqs. (1) and (2) yields

$$\varepsilon^0 = \sum_{n=0}^{N} \Delta_m C_n NLq_n^e = \sum_{n=0}^{N} B_{m_n} q_n^e$$

$$\chi = \sum_{n=0}^{N} \Delta_f C_n NLq_n^e = \sum_{n=0}^{N} B_{f_n} q_n^e \tag{9}$$

where the components of the membrane strains and changes of curvature are related to the vector of the element nodal displacement amplitudes in the referential system.

Using the orthogonality properties of trigonometric functions, considering also the applied loads expanded in terms of Fourier series, and following a standard procedure via the principle of virtual work, the stiffness matrix, load vector, and mass matrix for the nth harmonic can be represented as

$$K_n^e = K_{m_n}^e + K_{f_n}^e = \int_0^{2\pi}\int_0^1 \left(B_{m_n}^T D_m B_{m_n} + B_{f_n}^T D_f B_{f_n}\right) r\ell \, d\zeta \, d\theta \tag{10}$$

$$p_n^e = \int_0^{2\pi}\int_0^1 (N_n L)^T f_n^e r\ell \, d\zeta \, d\theta \tag{11}$$

$$M_n^e = \rho\int_0^{2\pi}\int_0^1 h\,(N_n L)^T (N_n L)\,\ell r \, d\zeta \, d\theta$$

$$+ \frac{\rho}{12}\int_0^{2\pi}\int_0^1 h^3 (R_n L)^T (R_n L)\,\ell r \, d\zeta \, d\theta \tag{12}$$

$$N_n = C_n N; \quad f_n^e = C_n N_f \bar{f}_n^e; \quad R_n = C_n \bar{R}_n \tag{13}$$

where D_m and D_f are the elasticity matrices for membrane and bending, r is the radial coordinate, ℓ is the length of generating line of the middle surface of the element, $\bar{f}_n^e$ is the vector of surface loads amplitudes, N_f and $\bar{R}_n$ are the matrices of shape functions or their derivatives, h is the thickness, ρ is the mass per unit of volume, and $\zeta = S/\ell$ is the element local natural coordinate.

The analytical derivative of the element stiffness matrix [Eq. (10)] for the nth harmonic with respect to a general variable b_k^* can be represented in a compact form as

$$\frac{\partial K_n^e}{\partial b_k^*} = \int_0^{2\pi}\int_0^1 \left\{\left[\left(B^T D\frac{\partial B}{\partial b_k^*}\right)^T + \left(B^T D\frac{\partial B}{\partial b_k^*}\right) + \left(B^T\frac{\partial D}{\partial b_k^*}B\right)\right]\ell r\right.$$

$$\left. + (B^T DB)\left(\frac{\partial r}{\partial b_k^*}\ell + r\frac{\partial \ell}{\partial b_k^*}\right)\right\} d\zeta \, d\theta \tag{14}$$

where

$$D = \begin{bmatrix} D_m & 0 \\ 0 & D_f \end{bmatrix}; \quad B = \begin{bmatrix} B_{m_n} \\ B_{f_n} \end{bmatrix} \tag{15}$$

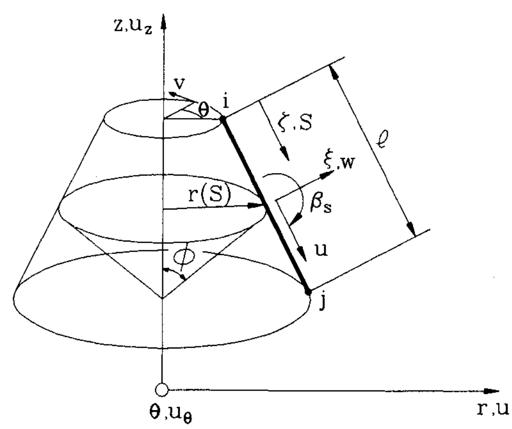

Fig. 1 Frustum-cone finite element; geometry and displacements.

The derivative of the element force vector is

$$\frac{\partial \boldsymbol{p}_n^e}{\partial \boldsymbol{b}_k^*} = \int_0^{2\pi}\int_0^1 \left\{ \left[\left(\frac{\partial \boldsymbol{L}^T}{\partial \boldsymbol{b}_k} \boldsymbol{L}_n^T \boldsymbol{f}_n^e \right) \right] \right.$$

$$+ \left(\boldsymbol{L}^T \frac{\partial \boldsymbol{N}_n^T}{\partial \boldsymbol{b}_k^*} \boldsymbol{f}_n^e \right) \left(\boldsymbol{L}^T \boldsymbol{N}_n^T \frac{\partial \boldsymbol{f}_n^e}{\partial \boldsymbol{b}_k^*} \right) \Bigg] \ell r$$

$$\left. + (\boldsymbol{L}^T \boldsymbol{N}_n^T \boldsymbol{f}_n^e) \left(\frac{\partial r}{\partial \boldsymbol{b}_k^*} \ell + r \frac{\partial \ell}{\partial \boldsymbol{b}_k^*} \right) \right\} \, d\zeta \, d\theta \tag{16}$$

The derivatives of the mass matrix are obtained in a similar way. The derivatives of the arguments are evaluated at each Gauss point, separately for membrane and bending, and numerical integration is used. Alternatively, when the design variables are radial coordinates, the derivatives of Eq. (14), the derivatives of the mass matrix and the integration of Eq. (11) and its derivatives $\partial p^e / \partial b_k^*$ are carried out using a symbolic manipulator. Full details are presented in Barbosa.[14]

When the design variables are thicknesses, the sensitivities of stiffness matrix $\boldsymbol{K}^e$ or mass matrix $\boldsymbol{M}^e$ are easily obtained. In fact, the mass matrix $\boldsymbol{M}^e$ depends explicitly on the thickness, whereas for the stiffness matrix $\boldsymbol{K}^e$ the dependence is only on constitutive matrices $\boldsymbol{D}_m$ and $\boldsymbol{D}_f$. Assuming the thickness constant within the element, one obtains:

$$\frac{\partial \boldsymbol{K}_n^e}{\partial h} = \frac{1}{h} \boldsymbol{K}_{m_n}^e + \frac{3}{h} \boldsymbol{K}_{f_n}^e \tag{17}$$

$$\frac{\partial \boldsymbol{M}_n^e}{\partial h} = \frac{1}{h} \boldsymbol{M}_{n_t}^e + \frac{3}{h} \boldsymbol{M}_{n_r}^e \tag{18}$$

where, respectively, $\boldsymbol{K}_{m_n}^e$, $\boldsymbol{K}_{f_n}^e$, $\boldsymbol{M}_{n_t}^e$, and $\boldsymbol{M}_{n_r}^e$ are the membrane and bending terms of the element stiffness matrix and the terms of element mass matrix due to translational and rotational inertia.

For nodal coordinates or when the thickness distribution varies within the element, the shape of the model is related through the linking relation[15]

$$\boldsymbol{s} = \boldsymbol{s}^c + \boldsymbol{T}\boldsymbol{b} \tag{19}$$

where $\boldsymbol{s}$ is the vector of dependent variables (thicknesses and/or radial nodal coordinates of the finite element model), $\boldsymbol{T}$ is the linking matrix that relates the vector of shape design variables $\boldsymbol{b}$ with the dependent variables, and $\boldsymbol{s}^c$ is a vector of constant terms.

With regard to shape design variables and considering the linking relation [Eq. (19)], the sensitivities of the element stiffness, mass, or load vector can also be obtained analytically through

$$\frac{\partial F^e}{\partial b_i} = \sum_{k=1}^{2} \frac{\partial F^e}{\partial b_k^*} \frac{\partial b_k^*}{\partial b_i} = \sum_{k=1}^{2} \frac{\partial F^e}{\partial b_k^*} T_{ki}^e \qquad i = 1, n \tag{20}$$

where F^e can be the stiffness and mass matrices or load vector of the eth element, and T_{ki}^e is related to the linking matrix $\boldsymbol{T}$ through the topological finite element code procedure, where b_k^* is the value of the element nodal variable concerned, namely, the nodal coordinates of the two ring node frustum conical element (r_k^e, z_k^e; k = 1,2).

For static constraints, the sensitivities are evaluated through the technique of adjoint structure, assuming that, for the nth harmonic, the structure satisfies the equilibrium equation

$$\boldsymbol{K}_n \lambda_{j_n} = z_{j_n} \tag{21}$$

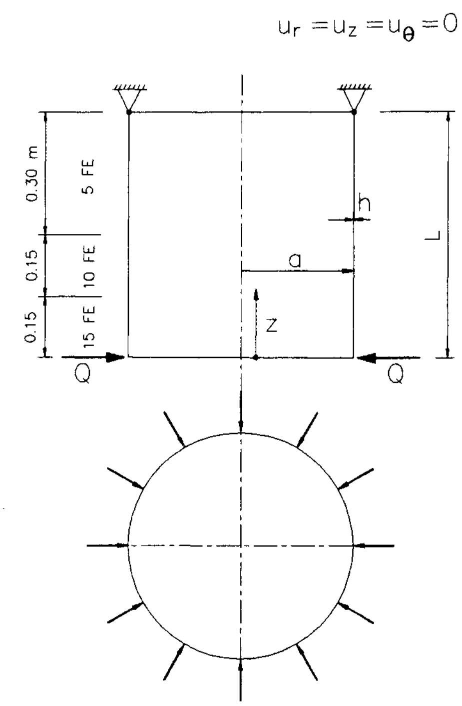

Fig. 2 Supported cylinder; geometry and load.

where $z_{j_n} = \partial g_{j_n} / \partial \boldsymbol{q}_n$ is the vector of adjoint forces, $\boldsymbol{q}_n$ is the vector of system degrees of freedom, and λ_{j_n} is the system adjoint degrees of freedom for the constraint g_{j_n}.

The sensitivities of a constraint function or the sensitivity of natural frequency with respect to a design variable are evaluated efficiently at an element level using equations

$$\frac{dg_j}{db_i} = \sum_{n=0}^{N} \left[\frac{\partial g_{j_n}}{\partial b_i} + \sum_{e \varepsilon E} \lambda_{j_n}^{e^T} \left(\frac{\partial \boldsymbol{p}_n^e}{\partial b_i} - \frac{\partial \boldsymbol{K}_n^e}{\partial b_i} \boldsymbol{q}_n^e \right) \right] \tag{22}$$

$$\frac{\partial \omega_k}{\partial b_i} = \frac{1}{2\omega_{k_n}} \sum_{e \varepsilon E} \boldsymbol{q}_{k_n}^{e^T} \left(\frac{\partial \boldsymbol{K}_n^e}{\partial b_i} - \omega_{k_n}^2 \frac{\partial \boldsymbol{M}_n^e}{\partial b_i} \right) \boldsymbol{q}_{k_n}^e \tag{23}$$

where E is the set of elements e that are affected by the design variable b_i, and N is the total number of harmonic terms. The element vectors λ_j^e, $\boldsymbol{q}^e$, and $\boldsymbol{q}_k^e$ are related to the system vectors λ_j, $\boldsymbol{q}$, and $\boldsymbol{q}_k$ of the nth harmonic, through the topological finite element code procedure.

Semianalytical Method

In this technique the vector of adjoint forces is obtained analytically, and the gradients of Eqs. (22) and (23), with terms of the type $\partial F / \partial b_i$, are evaluated by the forward finite difference (FFD) technique through the approximation

$$\frac{\partial F}{\partial b_i} \approx \frac{F(\boldsymbol{b} + \Delta \boldsymbol{b}) - F(\boldsymbol{b})}{\delta b_i} \tag{24}$$

where $\Delta \boldsymbol{b} = [0, \ldots, \delta b_i, \ldots, 0]$ and δb_i is a small perturbation. It should be noticed that to evaluate $F(\boldsymbol{b} + \Delta \boldsymbol{b})$ for shape optimization it is necessary to calculate the coordinate perturbations δr due to a design perturbation δb_i and these are carried out through the linking relation.

Finite Difference Technique

A global finite difference approach can be used as, for instance, FFD. In this case the sensitivity of a constraint with respect to a change δb_i in a design variable is given by

$$\frac{\mathrm{d}g_j}{\mathrm{d}b_i} \approx \frac{g_j(b_1, \ldots, b_i + \delta b_i, \ldots, b_n) - g_j(\boldsymbol{b})}{\delta b_i} \tag{25}$$

which needs one extra structural analysis for each design variable. Using central finite difference (CFD) the evaluation of sensitivities needs two extra structural analyses for each design variable, increasing the computational effort.

Constraints

Limit on Displacements

A constraint on a displacement is represented in normalized form by

$$g_j = \frac{q_f}{q_0} - 1 \leq 0 \tag{26}$$

where q_f is the real generalized displacement corresponding to system degree of freedom f, and q_0 is the maximum admissible generalized displacement.

Expanding q_f by Fourier series, one obtains the vector of adjoint forces for the nth harmonic as

$$z_{j_n} = \left[\frac{\partial g_{j_n}}{\partial q_1} \cdots \frac{\partial g_{j_n}}{\partial q_f} \cdots \frac{\partial g_{j_n}}{\partial q_p}\right]^T = \left[0 \ldots \frac{C_s}{q_0} \ldots 0\right]^T \tag{27}$$

where p is the total number of degrees of freedom, and $C_s = \cos n\theta$ or $C_s = \sin n\theta$ relating the corresponding degree of freedom. For a general arbitrary loading, these vectors are obtained easily for the antisymmetric terms. It should be noticed that the adjoint structure is identical to the real structure, and it is subjected to a force or moment of intensity C_s/q_0 on the corresponding degree of freedom where the displacement or rotation is limited.

Thus the sensitivity of a displacement constraint evaluated by Eq. (22) yields

$$\frac{\mathrm{d}g_j}{\mathrm{d}b_i} = \sum_{n=0}^{N} \sum_{e \epsilon E} \lambda_{j_n}^{e^T} \left(\frac{\partial \boldsymbol{p}_n^e}{\partial b_i} - \frac{\partial \boldsymbol{K}_n^e}{\partial b_i} \boldsymbol{q}_n^e\right) \tag{28}$$

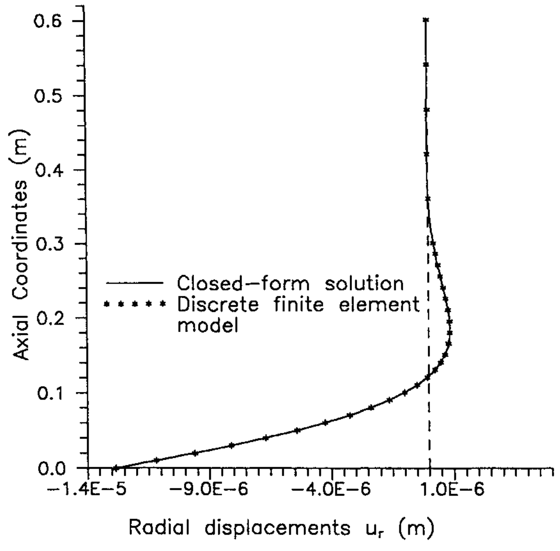

Fig. 3 Radial displacements distribution.

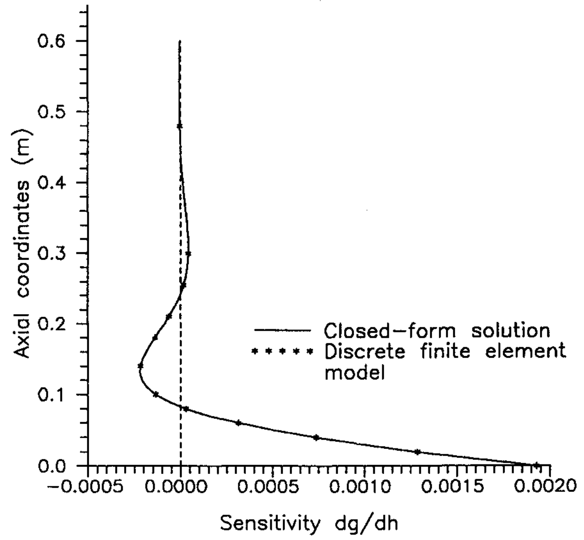

Fig. 4 Sensitivity distribution.

For arbitrary loading, the final value of the sensitivity is then obtained by adding the corresponding contribution of the symmetric and antisymmetric terms.

Limit on Stresses

Limit on a stress or an effective stress is represented by

$$g_j = \frac{\bar{\sigma}}{\sigma_0} - 1 \leq 0 \tag{29}$$

where σ_0 is the maximum allowable stress, which may be different for tension and compression, and σ is the stress component or the effective stress that one pretends to constraint. In the case of a meridional stress at the extreme fibers, the stress component is represented for the nth harmonic as

$$\bar{\sigma} = \sigma_{SS_n}^m \pm \sigma_{SS_n}^f \tag{30}$$

For example, given a stress constraint at Gauss point of element c, which corresponds to the adjoint load vector $z_{j_n}^c$, the system adjoint force vector for the nth harmonic is then

$$z_{j_n}^T = \left[0 \ldots z_{j_n}^c \ldots 0\right]^T \tag{31}$$

with

$$z_{j_n}^c = \frac{\cos n\theta}{\sigma_0}\left(\boldsymbol{A}_{n_1}^T \pm \boldsymbol{G}_{n_1}^T\right) \tag{32}$$

where

$$\frac{1}{h}\boldsymbol{D}_m \boldsymbol{B}_{m_n} \boldsymbol{q}_n^e = \left[\boldsymbol{A}_{n_1}\ \boldsymbol{A}_{n_2}\ \boldsymbol{A}_{n_3}\right]^T \boldsymbol{q}_n^e \quad \text{(membrane stresses)} \tag{33}$$

$$\frac{6}{h^2}\boldsymbol{D}_f \boldsymbol{B}_{f_n} \boldsymbol{q}_n^e = \left[\boldsymbol{G}_{n_1}\ \boldsymbol{G}_{n_2}\ \boldsymbol{G}_{n_3}\right]^T \boldsymbol{q}_n^e \quad \text{(bending stresses)} \tag{34}$$

Thus, for a pointwise limit on a stress, such as defined by Eq. (29), the sensitivity of stress constraint to thickness variation, evaluated by Eq. (22), yields

$$\frac{\mathrm{d}g_j}{\mathrm{d}h_i} = \sum_{n=0}^{N}\left(\frac{\sigma_{SS_n}^f}{\sigma_0 h} - \sum_{e \epsilon E} \lambda_{j_n}^{e^T} \frac{\partial \boldsymbol{K}_n^e}{\partial h_i} \boldsymbol{q}_n^e\right) \tag{35}$$

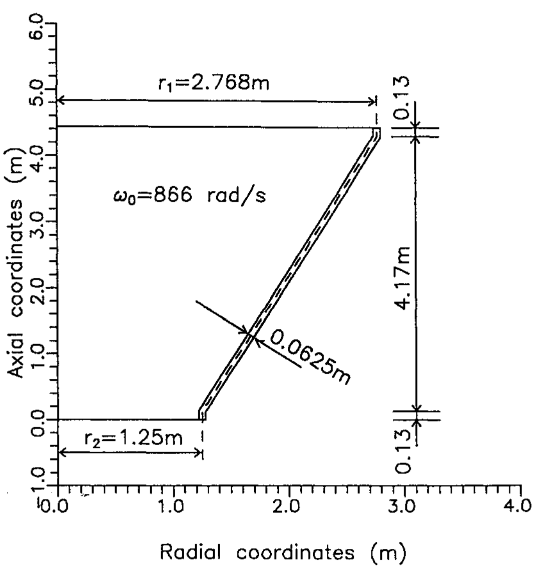

Fig. 5 Conical structure clamped at lower end.

where $\boldsymbol{h}$ is the thickness of the cth element where the constraint g_j has been imposed. If the design variable is a radial coordinate, then Eq. (22) can be represented as

$$\frac{\mathrm{d}g_j}{\mathrm{d}b_i} = \frac{1}{\sigma_0}\sum_{n=0}^{N}\left[\sum_{k=1}^{2}\frac{\partial}{\partial r_k^c}(\boldsymbol{A}_{n_1} \pm \boldsymbol{G}_{n_1})\,\boldsymbol{T}_{ki}^c\boldsymbol{q}_n^c\right.$$

$$\left. -\sum_{e\varepsilon E}\lambda_{j_n}^{e^T}\left(\frac{\partial \boldsymbol{p}_n^e}{\partial b_i} - \frac{\partial \boldsymbol{K}_n^e}{\partial b_i}\boldsymbol{q}_n^e\right)\right] \tag{36}$$

where the first terms of the second member of Eqs. (35) and (36) are evaluated only for the cth element where the stress constraint is imposed.

Limit on Natural Frequencies

A constraint in the natural frequency of mode k can be easily evaluated once the eigenvalue problem is solved. Considering a normalized constraint of the type

$$g_j = 1 - \frac{\omega_k}{\omega_0} \le 0 \tag{37}$$

the sensitivity given by Eq. (23) is evaluated as

$$\frac{\mathrm{d}g_j}{\mathrm{d}b_i} = -\frac{1}{2\omega_0\omega_{k_n}}\sum_{e\varepsilon E}\boldsymbol{q}_{k_n}^{e^T}\left(\frac{\partial \boldsymbol{K}_n^e}{\partial b_i} - \omega_{k_n}^2\frac{\partial \boldsymbol{M}_n^e}{\partial b_i}\right)\boldsymbol{q}_{k_n}^e \tag{38}$$

where ω_0 is the limiting natural frequency for mode k.

Limit on Volume of the Shell Material

For the present frustum-cone finite element, the volume of the shell material is given by

$$V = \sum_{e=1}^{I} V^e = \pi\sum_{e=1}^{I}\sqrt{(r_2^e - r_1^e)^2 + (z_2^e - z_1^e)^2}\,(r_1^e + r_2^e)\,h^e \tag{39}$$

where I is the total number of elements.

Imposing the initial volume V_0 of the shell material of the structure as constant and considering a normalized equality constraint of the type

$$g_j = \frac{V}{V_0} - 1 = 0 \tag{40}$$

the derivatives are easily obtained for constant thickness and radial coordinates, yielding, respectively,

$$\frac{\mathrm{d}g_j}{\mathrm{d}h_i} = \frac{\pi}{V_0}\sum_{e\varepsilon E}\ell(r_1^e + r_2^e) \tag{41}$$

$$\frac{\mathrm{d}g_j}{\mathrm{d}b_i} = \frac{\pi}{V_0}\sum_{e\varepsilon E}h^e\left\{\left[-\frac{(r_2^e)^2 - (r_1^e)^2}{\ell} + \ell\right]\boldsymbol{T}_{1i}^e\right.$$

$$\left. + \left[\frac{(r_2^e)^2 - (r_1^e)^2}{\ell} + \ell\right]\boldsymbol{T}_{2i}^e\right\} \tag{42}$$

The sensitivity of constraint on the enclosed volume of the structure is obtained in a similar way.

Optimal Design

The objective is the minimization of the volume V of the material, the maximization of natural frequency ω_k, the minimization of

Table 1 Sensitivities of fundamental frequency

Source	Perturbation	Sensitivities b_1	Sensitivities b_2
Analytical	——	−271.637	284.192
FFD	$0.001b_i$	−271.606	284.140
	$0.000000001b_i$	−271.720	284.192
	$0.0000001b_i$	−271.724	284.182
Semianalytical	$0.00001b_i$	−271.725	284.183
	$0.01b_i$	−272.109	285.353
	$0.05b_i$	−273.633	290.049

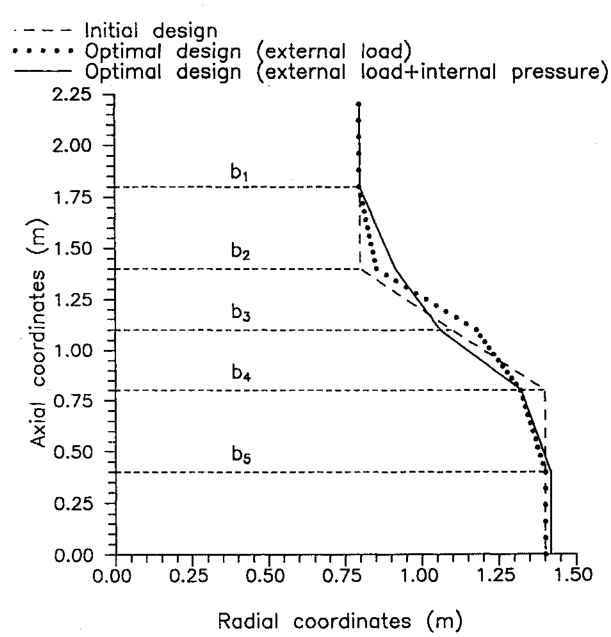

Fig. 6 Cylinder-cone-cylinder connection; initial and optimal designs.

Table 2 Sensitivities of a radial displacement constraint

		Sensitivities × 10^{-2}				
Source	Perturbation	b_1	b_2	b_3	b_4	b_5
Analytical	——	–0.06193	–0.9331	1.722	–0.7951	–0.3052
CFD	$0.0001b_i$	–0.06194	–0.9331	1.722	–0.7951	–0.3052
FFD	$0.0001b_i$	–0.06213	–0.9331	1.723	–0.7946	–0.3052
	$0.000000001b_i$	–0.06205	–0.9329	1.722	–0.7953	–0.3051
	$0.0000001b_i$	–0.06204	–0.9329	1.722	–0.7952	–0.3051
Semianalytical	$0.00001b_i$	–0.06191	–0.9323	1.723	–0.7947	–0.3051
	$0.001b_i$	–0.04853	–0.8755	1.821	–0.7441	–0.3073
	$0.01b_i$	0.0730	–0.3451	2.712	–0.3091	–0.3269
	$0.03b_i$	0.342	0.923	4.692	+0.511	–0.3686

Table 3 Sensitivities of a meridional stress using bound formulation

		Sensitivities × 10^{-2}				
Source	Perturbation	b_1	b_2	b_3	b_4	b_5
Analytical	——	0.6249	–0.3942	–1.981	1.741	0.01773
CFD	$0.0001b_i$	0.6263	–0.3894	–1.989	1.742	0.01759
FFD	$0.0001b_i$	0.6259	–0.3898	–1.988	1.743	0.01756
	$0.000000001b_i$	0.5951	–0.3209	–2.023	1.954	–0.1016
	$0.0000001b_i$	0.5951	–0.3209	–2.023	1.954	–0.1016
Semianalytical	$0.00001b_i$	0.5947	–0.3219	–2.024	1.953	–0.1018
	$0.001b_i$	0.5478	–0.4290	–2.150	1.872	–0.1229
	$0.01b_i$	0.1211	–0.1426	–3.281	1.163	–0.3139
	$0.03b_i$	–0.825	–0.3800	–5.752	–0.249	–0.7303

the maximum stress $\bar{\sigma}$, or the minimization of the maximum displacement q_f. The problem is stated as

$$\min V(b) \quad \text{or} \quad \max\omega_k(b) \quad \text{or} \quad \min[\max\bar{\sigma}(b)] \quad \text{or} \quad \min(\max q_f) \tag{43}$$

subject to

$$g_j(b) \le 0 \qquad j = 1, i \tag{44a}$$

$$g_k(b) = 0 \qquad k = i+1, m \tag{44b}$$

$$b_i^d \le b_i \le b_i^u \qquad i = 1, 2, \ldots, n \tag{44c}$$

where g_j are inequality constraints (such as displacement or stress); and g_k are equality constraints (enclosed volume of the structure or the volume of the shell material); b_i^d and b_i^u are the lower and upper limiting bounds of the design variables; and i, m, and n are the number of inequality constraints, total number of constraints, and total number of design variables, respectively.

Bound formulation[16] is used to solve the min-max problem. The problem is restated as a simple minimization problem in terms of a bound β on the value of max $\bar{\sigma}$

$$\min_D [\max\bar{\sigma}] \equiv \min \beta \tag{45}$$

Thus, in the domain D it is defined as an interval where the set of discrete values of maximum stress is calculated

$$(\beta - \Delta\beta) < \max\bar{\sigma}(b) \le \beta \qquad 0 < \Delta < 1 \tag{46}$$

where Δ is defined by the user, and it may be assigned different values during the optimization process. In the interval considered, there are different elements with maximum stresses or different values of maximum stresses along θ in the same element. Hence, to evaluate the objective function or the stress constraint, it is necessary to calculate the weight α_i^k of each value of maximum stress as

$$\alpha_i^k = 1 - \frac{\beta - \max\bar{\sigma}}{\Delta\beta} \tag{47}$$

Thus the weights of the M elements and L values along θ, where the maximum stress is in the interval considered, are normalized in the form

$$v_i^k = \frac{\alpha_i^k}{\sum_{k=1}^{M}\sum_{i=1}^{L}\alpha_i^k} \qquad \text{with} \qquad \sum_{k=1}^{M}\sum_{i=1}^{L} v_i^k = 1 \tag{48}$$

and the effective stress $\bar{\sigma}$ is represented as

$$\bar{\sigma} = \sum_{k=1}^{M}\sum_{i=1}^{L} v_i^k \sigma_i^k \tag{49}$$

In the package that was developed, using overlays, on a microcomputer AT IBM compatible, the main program calls the subprogram ADS[12] to solve the nonlinear mathematical programming problem, the subroutine OBJCON to calculate the objective function and the constraints, the subroutine GOBJCO to calculate the gradients of the objective function and constraints, and the subprogram FEMSOL to obtain the structural analysis of the optimal design.

The subprogram FEMSOL solves the system equation for statics considering arbitrary loading that is previously expanded by Fourier series and also the eigenvalue problem for dynamics. The gradients of constraints on displacements, stresses or natural frequency and the gradient of the objective function when the task is the minimization of maximum stresses, the maximization of natural frequency, or the minimization of maximum displacement are calculated in subroutine SENSIB that is included in FEMSOL.

Applications

Several illustrative examples using the proposed formulation are presented and discussed. The optimal designs shown in this paper were obtained using the modified feasible direction method implemented in ADS.

Supported Cylinder with End Shearing Force

The load, geometric, and material properties (Fig. 2) are Q = 1000 N/m, a = 1 m, h = 0.01 m, L = 0.6 m, E = 200 GPa (Young's modulus), and ν = 0.30 (Poisson's coefficient). A finite element model with 30 elements has been considered. The design variable is the thickness of the cylinder.

The radial displacement distribution of the Love-Kirchhoff analytical solution[13] is

$$u_r = -\frac{Q}{2\mu^3 D} e^{(-\mu z)} \cos(\mu z) \tag{50}$$

where

$$\mu = \left[\frac{3(1-\nu^2)}{a^2 h^2}\right]^{1/4}; \qquad D = \frac{Eh^3}{12(1-\nu^2)} \tag{51}$$

which compares very favorably with the present numerical solution (Fig. 3).

The sensitivity distribution obtained using the discrete finite element model with the analytical method has a very good agreement (Fig. 4) with the closed-form sensitivity obtained by differentiating the previous expression using a symbolic manipulator, yielding

$$\frac{du_r}{dh} = \frac{dg}{dh} = \frac{P_1 \cos(P_2)}{P_3 h^{5/2} E} - \frac{P_4 \cos(P_2)}{P_3 h^3 E} - \frac{P_4 \sin(P_2)}{P_3 h^3 E} \tag{52}$$

where

$$P_1 = 3.948 Q a^{3/2} (1-\nu^2)^{1/4}; \quad P_2 = \frac{1.316 z (1-\nu^2)^{1/4}}{(ah)^{1/2}}$$
$$P_3 = e^{\frac{1.316 z (1-\nu^2)^{1/4}}{\sqrt{ah}}}; \quad P_4 = 1.732 Q a z \sqrt{(1-\nu^2)} \tag{53}$$

Conical Structure Clamped at Lower End

To compare the three methods for a global constraint such as the fundamental natural frequency, we considered a conical shell clamped at the lower end with geometry shown in Fig. 5 and material properties E = 200 GPa (Young's modulus), ν = 0.15 (Poisson's coefficient), and ρ = 2410 Kg.m^{-3} (mass per unit volume). The structure has been modeled with 68 elements.

Table 1 shows, for the initial design, the sensitivity results of the fundamental frequency for the harmonic $n = 0$, with a good agreement between the three techniques, even for a perturbation of $0.05b_i$ for the semianalytical method.

Double-Supported Cylinder-Cone-Cylinder Connection

The geometry for the initial design (Fig. 6) and material properties are $b_1 = b_2 = 0.8$ m, $b_3 = 1.1$ m, $b_4 = b_5 = 1.4$ m, $h = 0.012$ m, H = 2.2 m (height of connection), E = 200 GPa, and ν = 0.3.

A finite element model with 50 elements has been considered. The design variables are five radial coordinates ($b_1,\ldots,b_5$). Tables 2 and 3 show the sensitivities for the initial design with respect to changes in the radial coordinates for a maximum displacement radial constraint and for meridional stress using bound formulation. The cylinder-cone-cylinder connection is submitted to an external surface load with the distribution represented in Fig. 7.

From Tables 2 and 3 it is observed that the analytical sensitivities for shape design sensitivities compare very favorably with the global finite element sensitivities obtained with the same model. As in axisymmetric loading,[17] it is also seen that the semianalytical sensitivities only compare favorably in some design variables for very small perturbations, since they are highly influenced by the perturbation used, due to the truncation on the finite difference method. The results obtained for b_5 using bound formulation as described in Eqs. (45–49) are in discrepancy for all of the perturbations used. Using central finite difference with the semianalytical method, the accuracy is not properly improved,[4] and the CPU time is increased. Some research is in progress to overcome these problems.[18]

A CPU ratio of 2.1 is achieved between the analytical vs semianalytical evaluation of sensitivities for a radial displacement con-

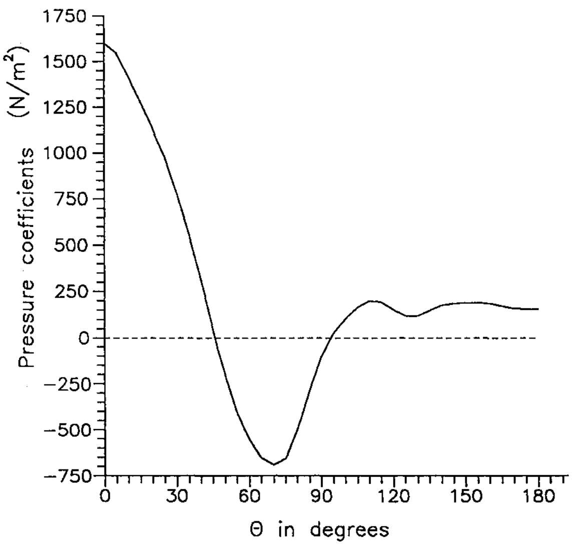

Fig. 7 Surface load variation.

Table 4 Sensitivities of fundamental frequency

	Sensitivities							
Source	h_1	h_2	h_3	h_4	h_5	h_6	h_7	b_1
Analytical	−809.3	−533.2	369.8	629.9	212.2	99.39	275.0	4.373
FFD	−809.0	−533.3	369.3	629.4	212.0	99.29	274.8	4.373

Table 5 Design variables for initial and optimal design

	Design variables, mm							
	h_1	h_2	h_3	h_4	h_5	h_6	h_7	b_1
Initial	12.0	12.0	12.0	12.0	12.0	12.0	12.0	1400
Optimal	05.0	05.0	12.3	48.4	11.2	09.5	15.7	1402

Table 6 Design variables for optimal design

	Design variables, mm						
	h_1	h_2	h_3	h_4	h_5	h_6	h_7
Mota Soares et al.	22.6	22.8	22.9	40.4	34.6	34.7	4.7
Present	21.0	22.4	24.5	43.0	32.3	32.5	4.0

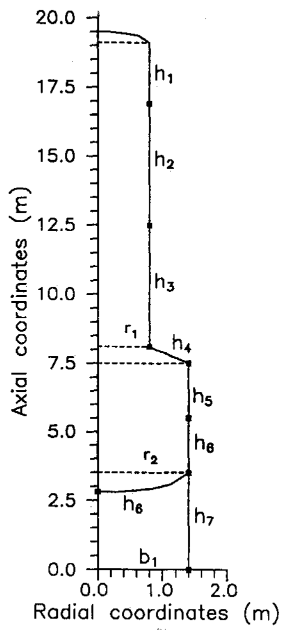

Fig. 8 Pressure vessel; initial design.

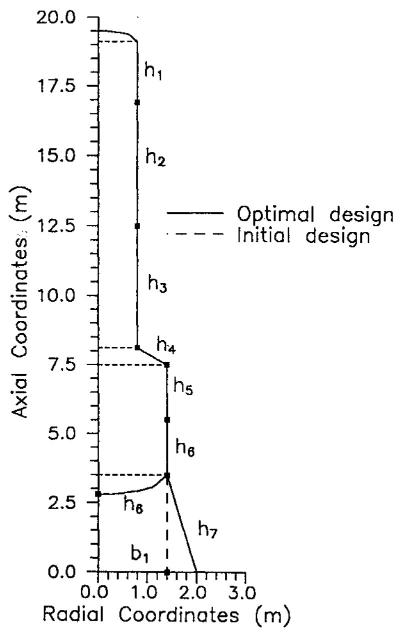

Fig. 9 Minimization of maximum displacement.

straint and a ratio of 1.9 for bound formulation. For axisymmetric loading and also using the semianalytical method as referential, we found a CPU ratio of 2.5 for the analytical method, a ratio of 3.2 for global forward finite difference, and a ratio of 5.4 for global central finite difference.

The double supported cylinder-cone-cylinder connection has been optimized first considering deflection and stress limits, respectively, of q_0 = 1 mm and σ_0 = 120 MPa. The optimal design is shown in Fig. 6 and is obtained with 35 iterations, 89 functions evaluations, and 19 gradient evaluations. We found a reduction in meridional stress, with regard to the initial design, of 39%. The maximum meridional stress in the model decreases from 0.638 to 0.388 MPa. Only the enclosed volume of the initial design (8.872 m^3), equality constraint, is activated. The model has also been optimized considering the surface load distribution (Fig. 7) and an internal pressure of 0.5 MPa. The optimal design (Fig. 6) is obtained with 8 iterations, 19 functions evaluations, and 3 gradient evaluations. In this case the maximum meridional stress in the model decreases from 117 to 79 MPa. It was used for bound formulation Δ = 0.2 for the first 10 evaluations, Δ = 0.1 for the next 20 evaluations, and Δ = 0.05 to the end of the problem.

Pressure Vessel

The last example shown is a pressure vessel with the same material properties (E = 210 GPa, ν = 0.3, ρ = 7800 $Kg.m^{-3}$) but different geometries. First we considered an initial design (Fig. 8) with r_1 = 0.8 m, r_2 = 1.4 m, h = 12 mm, and height H = 19.5 m. The structure has been modeled with 95 elements. The design variables are seven thicknesses ($h_1,\ldots,h_7$) and one radial coordinate b_1. Table 4 shows for the initial design the sensitivities of fundamental frequency. For FFD a perturbation of $0.001b_i$ was used.

The objective of the design is the maximization of lower fundamental frequency. It was used for the analysis five harmonic terms of Fourier series and four modes for each harmonic term. The optimal design was obtained in 5 iterations, 49 function evaluations, and 5 gradient evaluations. During the iteration process the volume of the shell material of the initial design (1.656 m^3) is an active constraint, and for thicknesses it used the interval $5 \le h_i \le 50$ mm for lower and upper bounds, respectively. The lower fundamental frequency is given for the first mode of harmonic term n = 1, and it is increased from 36 rad/s in the initial design to 63 rad/s in the optimal design. Table 5 shows the design variables for the optimal design.

The same geometry with thickness equal to 8 mm and the same design variables were used to minimize the maximum displacement in node 1 (r = 0, z = 19.5 m). As lower and upper bounds it used $5 \le h_i \le 12$ mm and $0.15 \le r_1 \le 2$ m. The pressure vessel was submitted to wind load (Fig. 7) and the displacements were calculated for θ = 0, 45, 60, 90, 135, and 180 deg. The optimal design (Fig. 9) was achieved in 2 iterations, 25 function evaluations, and 2 gradient evaluations. The design variables (seven thicknesses, and one radial coordinate) are set to the upper bounds in the final design, and the reduction on displacement was 8.3% (2.743 to 2.516 mm).

The last case shown is a pressure vessel with the same material properties but using different geometry with $h_1 = h_2 = h_3$ = 35 mm, h_4 = 45 mm, $h_5 = h_6 = h_7$ = 40 mm, r_1 = 0.4 m, r_2 = 0.65 m, and height H = 21.4 m. The pressure vessel was submitted to wind load (Fig. 7) and an internal pressure of 5.27 MPa. The design variables are seven thicknesses, and the objective of the design is the minimization of the volume of shell material, considering the maximum displacement and the maximum circumferential stress as constraints and a lower bound of 4 mm for the thickness. The optimal design is obtained in 7 iterations, 30 function evaluations, and 5 gradient evaluations, and it is in agreement with a simplified model used by Mota Soares[19] as shown in Table 6.

Conclusions

The results presented show that sensitivity analysis of statical and dynamic constraints of axisymmetric shells are efficiently and accurately obtained using the analytical method here described. When the design variables are thicknesses, all of the described techniques calculate the response sensitivities with accuracy. The same conclusion may be made for a global constraint (or objective function) such as the fundamental natural frequency.

From the observation of results, we can conclude that analytical sensitivities for shape design are more accurate than the semi-analytical sensitivities. Hence analytical sensitivities should be recommended for shape optimization of axisymmetric-type structures, although they are more difficult to obtain and more expensive in terms of CPU time when compared with semianalytical formulation.

Symbolic manipulators are powerful tools in the development of shape design sensitivities.

The semianalytical techniques for sensitivities of shape design variables cannot be very accurate even when central finite difference is used, and it will require a very small perturbation to obtain acceptable results. However, this perturbation can create problems of numerical stability.

The proposed methods are applied to several design problems and the numerical results show that the frustum-cone finite element used, the algorithms developed to obtained sensitivities and the modified method of feasible directions of ADS make promising tools to obtain optimal designs for axisymmetric laminate shell structures subjected to arbitrary loading.

Acknowledgments

The authors wish to thank JNICT—Junta Nacional de Investigação Científica e Tecnológica (Proj. C/MPF/531/90 and STRD/A/TPR/592/92), Fundação Calouste Gulbenkian, and FLAD-Fundação Luso Americana for their financial support.

References

[1]Zienkiewicz, O. C., *The Finite Element Method in Engineering Science*, 3rd ed., McGraw-Hill, London, 1977.

[2]Zienkiewicz, O. C., and Campbell, J. S., "Shape Optimization and Sequential Linear Programming," *Optimum Structural Design*, edited by R. H. Gallagher and O. C. Zienkiewicz, Wiley, London, 1973.

[3]Cheng, G., and Liu, Y., "A New Computation Scheme for Sensitivity Analysis," *Engineering Optimization*, Vol. 12, No. 3, 1987, pp. 219–234.

[4]Barthelemy, B., Chon, C. T., and Haftka, R. T., "Accuracy Problems Associated with Semi-Analytical Derivatives of Static Response," *Journal of Finite Elements in Analysis and Design*, Vol. 4, 1988, pp. 249–265.

[5]Haftka, R. T., and Kamat, M. P., "Finite Elements in Structural Design," *Computer Aided Optimal Design: Structural and Mechanical Systems*, edited by C. A. Mota Soares, Springer-Verlag, Berlin, 1987, pp. 241–270.

[6]Marcelin, J. L., and Trompette, P., "Optimal Shape Design of Thin Axisymmetric Shells," *Engineering Optimization*, Vol. 13, No. 2, 1988, pp. 108–117.

[7]Plaut, R. H., Johnson, L. W., and Parbery, R., "Optimal Form of Shallow Shells with Circular Boundary," *Transactions of the ASME*, Vol. 51, 1984, pp. 526–538.

[8]Chenais, D., "Shape Optimization in Shell Theory: Design Sensitivity of the Continuous Problem," *Engineering Optimization*, Vol. 11, No. 4, 1987, pp. 289–303.

[9]Mehrez, S., and Rousselet, B., "Analysis and Optimization of a Shell of Revolution," *Computer Aided Optimum Design of Structures: Applications*, edited by C. A. Brebbia and S. Hernandez, Computational Mechanics Publications, Springer-Verlag, Berlin, 1989, pp. 123–133.

[10]Bernadou, M., Palma, F. J., and Rousselet, B., "Shape Optimization of an Elastic Thin Shell Under Various Criteria," *Structural Optimization*, Vol. 3, No. 1, 1991, pp. 7–21.

[11]Noor, A. K., Elishakoff, I., and Hulbert, G., *Symbolic Computations and their Impact on Mechanics*, PVP-Vol. 205, American Society of Mechanical Engineers, New York, 1990.

[12]Vanderplaats, G. N., "ADS—A Fortran Program for Automated Design Synthesis, Version 2.01," Engineering Design Optimization, Inc., Santa Barbara, CA, Jan. 1987.

[13]Kraus, H., *Thin Elastic Shells*, Wiley, New York, 1967.

[14] Barbosa, J. I., "Computer Aided Optimum Design of Thin Axisymmetric Shells Structures," Ph.D. Thesis, Dept. of Mechanical Engineering, IST, Technical Univ. of Lisbon, Lisbon, Portugal, 1992 (in Portuguese).

[15]Vanderplaats, G. N., *Numerical Optimization Techniques for Engineering Design*, McGraw-Hill, New York, 1984.

[16]Taylor, J. E., and Bendsøe, M. P., "An Interpretation for Min-Max Structural Design Problems Including a Method for Relaxing Constraints," *International Journal of Solids and Structures*, Vol. 20, No. 4, 1984, pp. 301–314.

[17]Barbosa, J. I., Mota Soares, C. M., and Mota Soares, C. A., "Sensitivity Analysis and Shape Optimal Design of Axisymmetric Shell Structures," *Computing Systems in Engineering*, Vol. 2, No. 5/6, 1991, pp. 525–533.

[18]Olhoff, N., Rasmussen, J., and Lund, E., "A Method of 'Exact' Numerical Differentiation for Error Elimination in Finite-Element-Based Semi-Analytical Shape Sensitivity Analyses," *Mechanics of Structures and Machines*, Vol. 21, No. 1, 1993, pp. 1 – 66.

[19]Mota Soares, C. A., Mota Soares, C. M., and Mateus, H., "Optimal Design of Vertical Pressure Vessels with Supporting Cylindrical or Conical Skirt," *Journal of Engineering Optimization*, Vol. 11, No. 3/4, 1987, pp. 217–225.